

Faint galaxies, extragalactic background light, and the reionization of the Universe

Piero Madau

Space Telescope Science Institute, Baltimore, MD 21218

Abstract.

I review recent observational and theoretical progress in our understanding of the cosmic evolution of luminous sources. Largely due to a combination of deep *HST* imaging, Keck spectroscopy, and *COBE* far-IR background measurements, new constraints have emerged on the emission history of the galaxy population as a whole. Barring large systematic effects, the global ultraviolet, optical, near- and far-IR photometric properties of galaxies as a function of cosmic time cannot be reproduced by a simple stellar evolution model defined by a constant (comoving) star-formation density and a universal (Salpeter) IMF, and require instead a substantial increase in the stellar birthrate with lookback time. While the bulk of the stars present today appears to have formed relatively recently, the existence of a decline in the star-formation density above $z \approx 2$ remains uncertain. The history of the transition from the cosmic ‘dark age’ to a ionized universe populated with luminous sources can constrain the star formation activity at high redshifts. If stellar sources are responsible for photoionizing the intergalactic medium at $z \approx 5$, the rate of star formation at this epoch must be comparable or greater than the one inferred from optical observations of galaxies at $z \approx 3$. A population of dusty, Type II AGNs at $z \lesssim 2$ could make a significant contribution to the FIR background if the accretion efficiency is $\sim 10\%$.

INTRODUCTION

There is little doubt that the last few years have been exciting times in galaxy formation and evolution studies. The remarkable progress in our understanding of faint galaxy data made possible by the combination of HST deep imaging [62] and ground-based spectroscopy [35], [14], [56] has permitted to shed new light on the evolution of the stellar birthrate in the universe, to identify the epoch $1 \lesssim z \lesssim 2$ where most of the optical extragalactic background light was produced, and to set important constraints on galaxy evolution scenarios [41], [57], [3], [23]. The explosion in the quantity of information available on the high-redshift universe at optical wavelengths has been complemented by the detection of the far-IR/sub-mm background by DIRBE and FIRAS [28], [16]. The IR data have revealed the

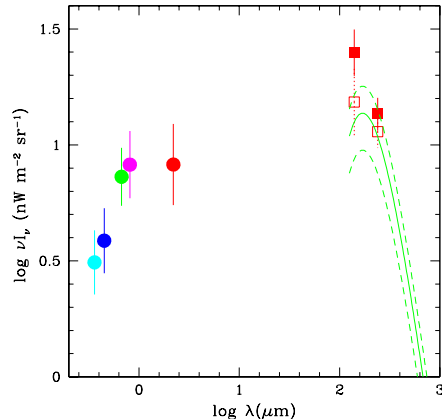


FIGURE 1. Spectrum of the extragalactic background light as derived from a compilation of ground-based and space-based galaxy counts in the U , B , V , I , and K -bands (*filled dots*), together with the FIRAS 125–5000 μm (*solid and dashed lines*) and DIRBE 140 and 240 μm (*filled squares*) detections. The *empty squares* show the DIRBE points after correction for WIM dust emission [32].

optically ‘hidden’ side of galaxy formation, and shown that a significant fraction of the energy released by stellar nucleosynthesis is re-emitted as thermal radiation by dust. The underlying goal of all these efforts is to understand the growth of cosmic structures and the mechanisms that shaped the Hubble sequence, and ultimately to map the transition from the cosmic ‘dark age’ to a ionized universe populated with luminous sources. While one of the important questions recently emerged is the nature (starbursts or AGNs?) and redshift distribution of the ultraluminous sub-mm sources discovered by *SCUBA* [30], [2], [36], of perhaps equal interest is the possible existence of a large population of faint galaxies still undetected at high- z , as the color-selected ground-based and *Hubble Deep Field* (HDF) samples include only the brightest and bluest star-forming objects. In hierarchical clustering cosmologies, high- z dwarfs and/or mini-quasars (i.e. an early generation of stars and accreting black holes in dark matter halos with circular velocities $v_c \sim 50 \text{ km s}^{-1}$) may actually be one of the main source of UV photons and heavy elements at early epochs [44], [25], [26].

In this talk I will focus on some of the open issues and controversies surrounding our present understanding of the history of the conversion of cold gas into stars within galaxies, and of the evolution with cosmic time of luminous sources in the universe. An Einstein-deSitter (EdS) universe ($\Omega_M = 1$, $\Omega_\Lambda = 0$) with $h = H_0/100 \text{ km s}^{-1} \text{ Mpc}^{-1} = 0.5$ will be adopted in the following.

OPTICAL/FIR BACKGROUND

The extragalactic background light (EBL) is an indicator of the total luminosity of the universe. It provides unique information on the evolution of cosmic structures at all epochs, as the cumulative emission from galactic systems and AGNs is expected to be recorded in this background. Figure 1 shows the optical EBL from known galaxies together with the recent *COBE* results. The value derived by integrating the galaxy counts [49] down to very faint magnitude levels [because of the flattening at faint magnitudes of the $N(m)$ differential counts most of the contribution to the optical EBL comes from relatively bright galaxies] implies a lower limit to the EBL intensity in the 0.3–2.2 μm interval of $I_{\text{opt}} \approx 12 \text{ nW m}^{-2} \text{ sr}^{-1}$.¹ When combined with the FIRAS and DIRBE measurements ($I_{\text{FIR}} \approx 16 \text{ nW m}^{-2} \text{ sr}^{-1}$ in the 125–5000 μm range), this gives an observed EBL intensity in excess of $28 \text{ nW m}^{-2} \text{ sr}^{-1}$. The correction factor needed to account for the residual emission in the 2.2 to 125 μm region is probably $\lesssim 2$ [13]. We shall see below how a population of dusty AGNs could make a significant contribution to the FIR background. In the rest of this talk I will adopt a conservative reference value for the total EBL intensity associated with star formation activity over the entire history of the universe of $I_{\text{EBL}} = 40 I_{40} \text{ nW m}^{-2} \text{ sr}^{-1}$.

COSMIC STAR FORMATION

It has become familiar to interpret recent observations of high-redshift sources via the comoving volume-averaged history of star formation. This is the mean over cosmic time of the stochastic, possibly short-lived star formation episodes of individual galaxies, and follows a relatively simple dependence on redshift. Its latest version, uncorrected for dust extinction, is plotted in Figure 2 (*left*). The measurements are based upon the rest-frame UV luminosity function (at 1500 and 2800 \AA), assumed to be from young stellar populations [38]. The prescription for a ‘correct’ de-reddening of these values has been the subject of an ongoing debate. Dust may play a role in obscuring the UV continuum of Canada-France Redshift Survey (CFRS, $0.3 < z < 1$) and Lyman-break ($z \approx 3$) galaxies, as their colors are too red to be fitted with an evolving stellar population and a Salpeter initial mass function (IMF) [41]. The fiducial model of [41] had an upward correction factor of 1.4 at 2800 \AA , and 2.1 at 1500 \AA . Much larger corrections have been argued for by [50] ($\times 10$ at $z = 1$), [43] ($\times 15$ at $z = 3$), and [51] ($\times 16$ at $z > 2$). As noted already by [38] and [41], a consequence of such large extinction values is the possible overproduction of metals and red light at low redshifts. Most recently, the evidence for more moderate extinction corrections has included measurements of star-formation rates (SFR) from Balmer lines by [59] ($\times 2$ at $z = 0.2$), [21]

¹) Note that the direct detection of the optical EBL at 3000, 5500, and 8000 \AA derived from *HST* data by [5] implies values that are about a factor of two higher than the integrated light from galaxy counts.

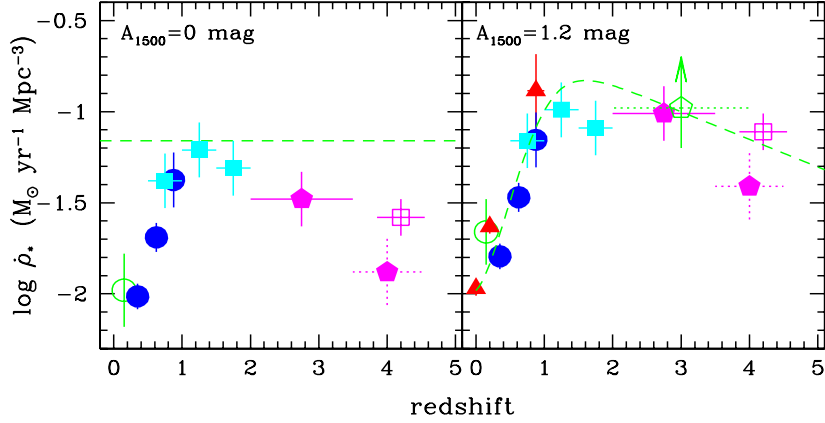


FIGURE 2. *Left:* Mean comoving density of star formation as a function of cosmic time. The data points with error bars have been inferred from the UV-continuum luminosity densities of [35] (*filled dots*), [10] (*filled squares*), [41] (*filled pentagons*), [60] (*empty dot*), and [58] (*empty square*). The *dotted line* shows the fiducial rate, $\langle \dot{\rho}_* \rangle = 0.054 \text{ M}_\odot \text{ yr}^{-1} \text{ Mpc}^{-3}$, required to generate the observed EBL. *Right:* dust corrected values ($A_{1500} = 1.2 \text{ mag}$, SMC-type dust in a foreground screen). The $\text{H}\alpha$ determinations of [19], [59], and [21] (*filled triangles*), together with the SCUBA lower limit [30] (*empty pentagon*) have been added for comparison.

($\times 3.1 \pm 0.4$ at $z = 1$), and [48] ($\times 2 - 6$ at $z = 3$). *ISO* follow-up of CFRS fields [17] has shown that the star-formation density derived by FIR fluxes ($\times 2.3 \pm 0.7$ at $0 \leq z \leq 1$) is about 3.5 times lower than in [50]. Figure 2 (*right*) depicts an extinction-corrected (with $A_{1500} = 1.2 \text{ mag}$, 0.4 mag higher than in [41]) version of the same plot. The best-fit cosmic star formation history (shown by the *dashed-line*) with such a universal correction produces a total EBL of $37 \text{ nW m}^{-2} \text{ sr}^{-1}$. About 65% of this is radiated in the UV+optical+near-IR between 0.1 and $5 \mu\text{m}$; the total amount of starlight that is absorbed by dust and reprocessed in the far-IR is $13 \text{ nW m}^{-2} \text{ sr}^{-1}$. Because of the uncertainties associated with the incompleteness of the data sets, photometric redshift technique, dust reddening, and UV-to-SFR conversion, these numbers are only meant to be indicative. On the other hand, this very simple model is not in obvious disagreement with any of the observations, and is able, in particular, to provide a reasonable estimate of the galaxy optical and near-IR luminosity density.

STELLAR BARYON BUDGET

With the help of some simple stellar population synthesis tools it is possible at this stage to make an estimate of the stellar mass density that produced the integrated light observed today. The total *bolometric* luminosity of a simple stellar population (a single generation of coeval stars) having mass M can be well approximated by a power-law with time for all ages $t \gtrsim 100 \text{ Myr}$,

$$L(t) = 1.3 L_{\odot} \frac{M}{M_{\odot}} \left(\frac{t}{1 \text{ Gyr}} \right)^{-0.8} \quad (1)$$

(cf. [8]), where we have assumed solar metallicity and a Salpeter IMF truncated at 0.1 and $125 M_{\odot}$. In a stellar system with arbitrary star-formation rate per unit cosmological volume, $\dot{\rho}_*$, the comoving bolometric emissivity at time t is given by the convolution integral

$$\rho_{\text{bol}}(t) = \int_0^t L(\tau) \dot{\rho}_*(t - \tau) d\tau. \quad (2)$$

The total background light observed at Earth ($t = t_H$) is

$$I_{\text{EBL}} = \frac{c}{4\pi} \int_0^{t_H} \frac{\rho_{\text{bol}}(t)}{1+z} dt, \quad (3)$$

where the factor $(1+z)$ at the denominator is lost to cosmic expansion when converting from observed to radiated (comoving) luminosity density. From the above equations it is easy to derive in a EdS cosmology

$$I_{\text{EBL}} = 740 \text{ nW m}^{-2} \text{ sr}^{-1} \left\langle \frac{\dot{\rho}_*}{M_{\odot} \text{ yr}^{-1} \text{ Mpc}^{-3}} \right\rangle \left(\frac{t_H}{13 \text{ Gyr}} \right)^{1.87}. \quad (4)$$

The observations shown in Figure 1 therefore imply a “fiducial” mean star formation density of $\langle \dot{\rho}_* \rangle = 0.054 I_{40} M_{\odot} \text{ yr}^{-1} \text{ Mpc}^{-3}$. In the instantaneous recycling approximation, the total stellar mass density observed today is

$$\rho_*(t_H) = (1 - R) \int_0^{t_H} \dot{\rho}_*(t) dt \approx 5 \times 10^8 I_{40} M_{\odot} \text{ Mpc}^{-3} \quad (5)$$

(corresponding to $\Omega_* = 0.007 I_{40}$), where R is the mass fraction of a generation of stars that is returned to the interstellar medium, $R \approx 0.3$ for a Salpeter IMF. The optical/FIR background therefore requires that about 10% of the nucleosynthetic baryons today [7] are in the forms of stars and their remnants. The predicted stellar mass-to-blue light ratio is $\langle M/L_B \rangle \approx 5$. These values are quite sensitive to the lower-mass cutoff of the IMF, as very-low mass stars can contribute significantly to the mass but not to the integrated light of the whole stellar population. A lower cutoff of $0.5 M_{\odot}$ instead of the $0.1 M_{\odot}$ adopted would decrease the mass-to-light ratio (and Ω_*) by a factor of 1.9 for a Salpeter function.

TWO SIMPLE MODELS

Based on the agreement between the $z \approx 3$ and $z \approx 4$ luminosity functions at the bright end, it has been recently argued [58] that the decline in the luminosity density of faint HDF Lyman-break galaxies observed in the same redshift interval

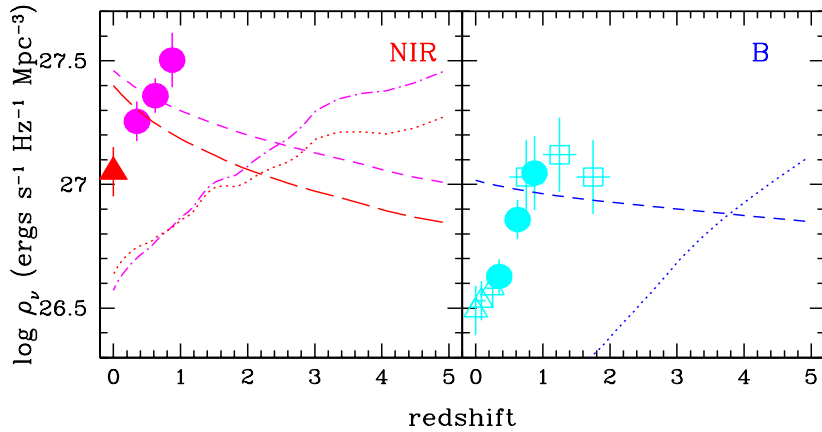


FIGURE 3. *Left:* Synthetic evolution of the near-IR luminosity density at rest-frame wavelengths of 1.0 (*long-dashed line*) and 2.2 μm (*short-dashed line*). The model assumes a constant star-formation rate of $\dot{\rho}_* = 0.054 \text{ M}_\odot \text{ yr}^{-1} \text{ Mpc}^{-3}$ (Salpeter IMF). The *dotted* (2.2 μm) and *dash-dotted* (1.0 μm) curves show the emissivity of a simple stellar population with formation redshift $z_{\text{on}} = 5$, and total mass equal to the mass observed in spheroids today [18]. The data points are taken from [35] (*filled dots*) and [20] (*filled triangle*). *Right:* Same but in the *B*-band. The data points are taken from [35] (*filled dots*), [14] (*empty triangles*), and [10] (*empty squares*).

[38] may not be real, but simply due to sample variance in the HDF. When extinction corrections are applied, the emissivity per unit comoving volume due to star formation may then remain essentially flat for all redshift $z \gtrsim 1$ (see Fig. 2). While this has obvious implications for hierarchical models of structure formation, the epoch of first light, and the reionization of the intergalactic medium (IGM), it is also interesting to speculate on the possibility of a constant star-formation density at *all* epochs $0 \leq z \leq 5$, as recently advocated by [47]. Figure 3 shows the time evolution of the blue and near-IR rest-frame luminosity density of a stellar population characterized by a Salpeter IMF, solar metallicity, and a (constant) star-formation rate of $\dot{\rho}_* = 0.054 \text{ M}_\odot \text{ yr}^{-1} \text{ Mpc}^{-3}$ (needed to produce the observed EBL). The predicted evolution appears to be a poor match to the observations: it overpredicts the local *B* and *K*-band luminosity densities, and underpredicts the 1 μm emissivity at $z \approx 1$ from the CFRS survey. ²

At the other extreme, we know from stellar population studies that about half of the present-day stars are contained in spheroidal systems, i.e. elliptical galaxies and spiral galaxy bulges, and that these stars formed early and rapidly [4]. The expected rest-frame blue and near-IR emissivity of a simple stellar population with formation redshift $z_{\text{on}} = 5$ and total mass density equal to the mass in spheroids

²⁾ The near-IR light is dominated by near-solar mass evolved stars, the progenitors of which make up the bulk of a galaxy's stellar mass, and is more sensitive to the past star-formation history than the blue light.

observed today (see below) is shown in Figure 3. *HST*-NICMOS deep observations may be able to test similar scenarios for the formation of elliptical galaxies at early times.

TYPE II AGNS

Recent dynamical evidence indicates that supermassive black holes reside at the center of most nearby galaxies. The available data (about 30 objects) show a strong correlation (but with a large scatter) between bulge and black hole mass [42], with $M_{\text{bh}} = 0.006 M_{\text{bulge}}$ as a best-fit. The total mass density in spheroids today is $\Omega_{\text{bulge}} = 0.0036^{+0.0024}_{-0.0017}$ [18], implying a mean mass density of dead quasars

$$\rho_{\text{bh}} = 1.5^{+1.0}_{-0.7} \times 10^6 \text{ M}_{\odot} \text{ Mpc}^{-3}. \quad (6)$$

Noting that the observed energy density from all quasars is equal to the emitted energy divided by the average quasar redshift [63], the total contribution to the EBL from accretion onto black holes is

$$I_{\text{bh}} = \frac{c^3}{4\pi} \frac{\eta \rho_{\text{bh}}}{\langle 1+z \rangle} \approx 18 \text{ nW m}^{-2} \text{ sr}^{-1} \eta_{0.1} \langle 1+z \rangle^{-1}, \quad (7)$$

where $\eta_{0.1}$ is the efficiency for transforming accreted rest-mass energy into radiation (in units of 10%). A population of AGNs at (say) $z \sim 1.5$ could then make a significant contribution to the FIR background if dust-obscured accretion onto supermassive black holes is an efficient process [24], [15]. It is interesting to note in this context that a population of AGNs with strong intrinsic absorption (Type II quasars) is actually invoked in many current models for the X-ray background [37], [9].

SOURCES OF IONIZING RADIATION

The application of the Gunn-Peterson constraint on the amount of smoothly distributed neutral material along the line of sight to distant objects requires the hydrogen component of the diffuse IGM to have been highly ionized by $z \approx 5$ [53], and the helium component by $z \approx 2.5$ [12]. From QSO absorption studies we also know that neutral hydrogen at early epochs accounts for only a small fraction, $\sim 10\%$, of the nucleosynthetic baryons [33]. It thus appears that substantial sources of ultraviolet photons were present at $z \gtrsim 5$, perhaps low-luminosity quasars [26] or a first generation of stars in virialized dark matter halos with $T_{\text{vir}} \sim 10^4 - 10^5 \text{ K}$ [46], [25], [44]. Early star formation provides a possible explanation for the widespread existence of heavy elements in the IGM [11], while reionization by QSOs may produce a detectable signal in the radio extragalactic background at meter wavelengths [40]. Establishing the character of cosmological ionizing sources is an

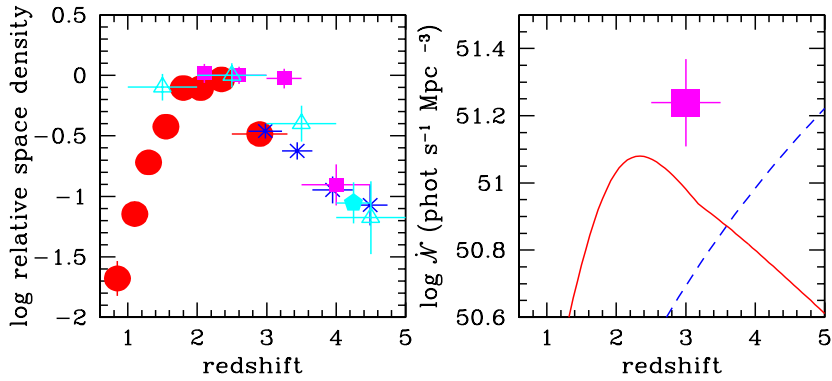


FIGURE 4. *Left:* comoving space density of bright QSOs as a function of redshift. The data points with error bars are taken from [27] (*filled dots*), [61] (*filled squares*), [52] (*crosses*), and [31] (*filled pentagon*). The *empty triangles* show the space density of the Parkes flat-spectrum radio-loud quasars with $P > 7.2 \times 10^{26} \text{ W Hz}^{-1} \text{ sr}^{-1}$ [29]. *Right:* comoving emission rate of hydrogen Lyman-continuum photons (*solid line*) from QSOs, compared with the minimum rate (*dashed line*) which is needed to fully ionize a fast recombining (with ionized gas clumping factor $C = 30$) EdS universe with $\Omega_b h^2 = 0.02$. Models based on photoionization by quasar sources appear to fall short at $z \sim 5$. The data point shows the estimated contribution of star-forming galaxies at $z \approx 3$, assuming that the fraction of Lyman continuum photons which escapes the galaxy H I layers into the intergalactic medium is $f_{\text{esc}} = 0.5$ (see [39] for details).

efficient way to constrain competing models for structure formation in the universe, and to study the collapse and cooling of small mass objects at early epochs.

What keeps the universe ionized at $z = 5$? The problem can be simplified by noting that the *breakthrough epoch* (when all radiation sources can see each other in the Lyman continuum) occurs much later in the universe than the *overlap epoch* (when individual ionized zones become simply connected and every point in space is exposed to ionizing radiation). This implies that at high redshifts the ionization equilibrium is actually determined by the *instantaneous* UV production rate [39]. The fact that the IGM is rather clumpy and still optically thick at overlapping, coupled to recent observations of a rapid decline in the space density of radio-loud quasars and of a large population of star-forming galaxies at $z \gtrsim 3$, has some interesting implications for rival ionization scenarios and for the star formation activity at $< 3 < z < 5$.

The existence of a decline in the space density of bright quasars at redshifts beyond ~ 3 was first suggested by [45], and has been since then the subject of a long-standing debate. In recent years, several optical surveys have consistently provided new evidence for a turnover in the QSO counts [27], [61], [52], [31]. The interpretation of the drop-off observed in optically selected samples is equivocal, however, because of the possible bias introduced by dust obscuration arising from intervening systems. Radio emission, on the other hand, is unaffected by dust, and it has recently been shown [54] that the space density of radio-loud quasars also decreases strongly for $z > 3$. This argues that the turnover is indeed real and that dust along the line of sight has a minimal effect on optically-selected QSOs (Figure 4, *left*). The QSO emission rate (corrected for incompleteness) of hydrogen ionizing photons per unit comoving volume is shown in Figure 4 (*right*) [39].

Galaxies with ongoing star-formation are another obvious source of Lyman continuum photons. Since the rest-frame UV continuum at 1500 \AA (redshifted into the visible band for a source at $z \approx 3$) is dominated by the same short-lived, massive stars which are responsible for the emission of photons shortward of the Lyman edge, the needed conversion factor, about one ionizing photon every 10 photons at 1500 \AA , is fairly insensitive to the assumed IMF and is independent of the galaxy history for $t \gg 10^7 \text{ yr}$. Figure 4 (*right*) shows the estimated Lyman-continuum luminosity density of galaxies at $z \approx 3$.³ The data point assumes a value of $f_{\text{esc}} = 0.5$ for the unknown fraction of ionizing photons which escapes the galaxy H I layers into the intergalactic medium. A substantial population of dwarf galaxies below the detection threshold, i.e. having star-formation rates $< 0.3 M_{\odot} \text{ yr}^{-1}$, and with a space density in excess of that predicted by extrapolating to faint magnitudes the best-fit Schechter function, may be expected to form at early times in hierarchical clustering models, and has been recently proposed by [44] and [39] as a possible candidate for photoionizing the IGM at these epochs. One should note that, while highly reddened galaxies at high redshifts would be missed by the dropout color

³) At all ages $\gtrsim 0.1 \text{ Gyr}$ one has $L(1500)/L(912) \approx 6$ for a Salpeter mass function and constant SFR [6]. This number neglects any correction for intrinsic H I absorption.

technique (which isolates sources that have blue colors in the optical and a sharp drop in the rest-frame UV), it seems unlikely that very dusty objects (with $f_{\text{esc}} \ll 1$) would contribute in any significant manner to the ionizing metagalactic flux.

REIONIZATION OF THE IGM

When an isolated point source of ionizing radiation turns on, the ionized volume initially grows in size at a rate fixed by the emission of UV photons, and an ionization front separating the H II and H I regions propagates into the neutral gas. Most photons travel freely in the ionized bubble, and are absorbed in a transition layer. The evolution of an expanding H II region is governed by the equation

$$\frac{dV_I}{dt} - 3HV_I = \frac{\dot{N}_{\text{ion}}}{\bar{n}_{\text{H}}} - \frac{V_I}{\bar{t}_{\text{rec}}}, \quad (8)$$

where V_I is the proper volume of the ionized zone, \dot{N}_{ion} is the number of ionizing photons emitted by the central source per unit time, \bar{n}_{H} is the mean hydrogen density of the expanding IGM, H is the Hubble constant, and \bar{t}_{rec} is the hydrogen mean recombination timescale,

$$\bar{t}_{\text{rec}} = [(1 + 2\chi)\bar{n}_{\text{H}}\alpha_B C]^{-1} = 0.3 \text{ Gyr} \left(\frac{\Omega_b h^2}{0.02}\right)^{-1} \left(\frac{1+z}{4}\right)^{-3} C_{30}^{-1}. \quad (9)$$

One should point out that the use of a volume-averaged clumping factor, C , in the recombination timescale is only justified when the size of the H II region is large compared to the scale of the clumping, so that the effect of many clumps (filaments) within the ionized volume can be averaged over (see Figure 5). Across the I-front the degree of ionization changes sharply on a distance of the order of the mean free path of an ionizing photon. When $\bar{t}_{\text{rec}} \ll t$, the growth of the H II region is slowed down by recombinations in the highly inhomogeneous medium, and its evolution can be decoupled from the expansion of the universe. Just like in the static case, the ionized bubble will fill its time-varying Strömngren sphere after a few recombination timescales,

$$V_I = \frac{\dot{N}_{\text{ion}}\bar{t}_{\text{rec}}}{\bar{n}_{\text{H}}}(1 - e^{-t/\bar{t}_{\text{rec}}}). \quad (10)$$

In analogy with the individual H II region case, it can be shown that hydrogen component in a highly inhomogeneous universe is completely reionized when the number of photons emitted above 1 ryd in one recombination time equals the mean number of hydrogen atoms [39]. At any given epoch there is a critical value for the photon emission rate per unit cosmological comoving volume,

$$\dot{N}_{\text{ion}}(z) = \frac{\bar{n}_{\text{H}}(0)}{\bar{t}_{\text{rec}}(z)} = (10^{51.2} \text{ s}^{-1} \text{ Mpc}^{-3}) C_{30} \left(\frac{1+z}{6}\right)^3 \left(\frac{\Omega_b h^2}{0.02}\right)^2, \quad (11)$$

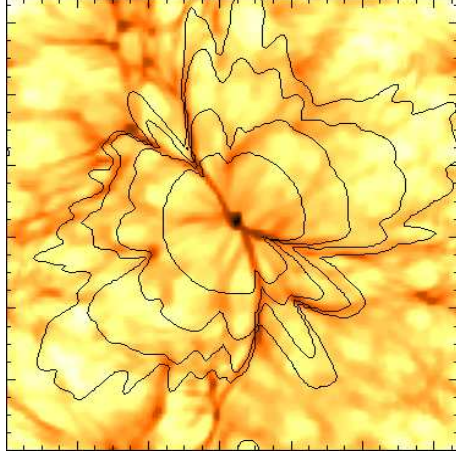


FIGURE 5. Propagation of an ionization front in a 128^3 cosmological density field produced by a mini-quasar with $\dot{N} = 5 \times 10^{53} \text{ s}^{-1}$. The box length is 2.4 comoving Mpc. The quasar is turned on at the densest cell, which is found in a virialized halo of total mass $1.3 \times 10^{11} M_{\odot}$. The solid contours give the position of the I-front at 0.15, 0.25, 0.38, and 0.57 Myr after the quasar has switched on at $z = 7$. The underlying greyscale image indicates the initial H I density field. (From [1].)

independently of the (unknown) previous emission history of the universe: only rates above this value will provide enough UV photons to ionize the IGM by that epoch. One can then compare our estimate of $\dot{\mathcal{N}}_{\text{ion}}$ to the estimated contribution from QSOs and star-forming galaxies. The uncertainty on this critical rate is difficult to estimate, as it depends on the clumpiness of the IGM (scaled in the expression above to the value inferred at $z = 5$ from numerical simulations [22]) and the nucleosynthesis constrained baryon density. The evolution of the critical rate as a function of redshift is plotted in Figure 4 (*right*). While $\dot{\mathcal{N}}_{\text{ion}}$ is comparable to the quasar contribution at $z \gtrsim 3$, there is some indication of a deficit of Lyman continuum photons at $z = 5$. For bright, massive galaxies to produce enough UV radiation at $z = 5$, their space density would have to be comparable to the one observed at $z \approx 3$, with most ionizing photons being able to escape freely from the regions of star formation into the IGM. This scenario may be in conflict with direct observations of local starbursts below the Lyman limit showing that at most a few percent of the stellar ionizing radiation produced by these luminous sources actually escapes into the IGM [34].⁴

It is interesting to convert the derived value of $\dot{\mathcal{N}}_{\text{ion}}$ into a “minimum” SFR per unit (comoving) volume, $\dot{\rho}_*$ (hereafter we assume $\Omega_b h^2 = 0.02$ and $C = 30$):

$$\dot{\rho}_*(z) = \dot{\mathcal{N}}_{\text{ion}}(z) \times 10^{-53.1} f_{\text{esc}}^{-1} \approx 0.013 f_{\text{esc}}^{-1} \left(\frac{1+z}{6} \right)^3 M_{\odot} \text{ yr}^{-1} \text{ Mpc}^{-3}. \quad (12)$$

⁴) Note that, at $z = 3$, Lyman-break galaxies would radiate more ionizing photons than QSOs for $f_{\text{esc}} \gtrsim 30\%$.

The star formation density given in the equation above is comparable with the value directly “observed” (i.e., uncorrected for dust reddening) at $z \approx 3$ [41]. The conversion factor assumes a Salpeter IMF with solar metallicity, and has been computed using a population synthesis code [6]. It can be understood by noting that, for each $1 M_{\odot}$ of stars formed, 8% goes into massive stars with $M > 20M_{\odot}$ that dominate the Lyman continuum luminosity of a stellar population. At the end of the C-burning phase, roughly half of the initial mass is converted into helium and carbon, with a mass fraction released as radiation of 0.007. About 25% of the energy radiated away goes into ionizing photons of mean energy 20 eV. For each $1 M_{\odot}$ of stars formed every year, we then expect

$$\frac{0.08 \times 0.5 \times 0.007 \times 0.25 \times M_{\odot} c^2}{20 \text{ eV}} \frac{1}{1 \text{ yr}} \sim 10^{53} \text{ phot s}^{-1} \quad (13)$$

to be emitted shortward of 1 ryd.

REFERENCES

1. Abel, T., Norman, M. L., & Madau, P. 1998, preprint (astro-ph/9812151)
2. Barger, A. J., et al. 1998, *Nature*, 394, 248
3. Baugh, C. M., et al. 1998, *ApJ*, 498, 504
4. Bernardi, M., et al. 1998, *ApJ*, 508, L143
5. Bernstein, R. A. 1998, preprint
6. Bruzual, A. C., & Charlot, S. 1999, in preparation
7. Burles, S., & Tytler, D. 1998, preprint (astro-ph/9803071)
8. Buzzoni, A. 1995, *ApJS*, 98, 69
9. Comastri, A., et al. 1995, *A&A*, 296, 1
10. Connolly, A. J., et al. 1997, *ApJ*, 486, L11
11. Cowie, L. L., et al. 1995, *AJ*, 109, 1522
12. Davidsen, A. F., Kriss, G. A., & Zheng, W. 1996, *Nature*, 380, 47
13. Dwek, E., et al. 1998, *ApJ*, 508, 106
14. Ellis, R. S., et al. 1996, *MNRAS*, 280, 235
15. Fabian, A. C., & Iwasawa, K. 1999, *MNRAS*, in press
16. Fixsen, D. J., et al. 1998, *ApJ*, 508, 123
17. Flores, H., et al. 1998, *ApJ*, in press (astro-ph/9811202)
18. Fukugita, M., Hogan, C. J., & Peebles, P. J. E. 1998, *ApJ*, 503, 518
19. Gallego, J., et al. 1995, *ApJ*, 455, L1
20. Gardner, J. P., et al. B. E. 1997, *ApJ*, 480, L99
21. Glazebrook, K., et al. 1998, *MNRAS*, submitted (astro-ph/9808276)
22. Gnedin, N. Y., & Ostriker, J. P. 1997, *ApJ*, 486, 581
23. Guiderdoni, B., et al. 1997, *Nature*, 390, 257
24. Haehnelt, M. G., Natarajan, P., & Rees, M. J. 1998, *MNRAS*, 300, 817
25. Haiman, Z., & Loeb, A. 1997, *ApJ*, 483, 21
26. Haiman, Z., & Loeb, A. 1998, *ApJ*, 503, 505
27. Hartwick, F. D. A., & Schade, D. 1990, *ARA&A*, 28, 437

28. Hauser, M. G., et al. 1998, *ApJ*, 508, 25
29. Hook, I. M., Shaver, P. A., & McMahon, R. G. 1998, in *The Young Universe: Galaxy Formation and Evolution at Intermediate and High Redshift*, ed. S. D'Odorico, A. Fontana, & E. Giallongo (San Francisco: ASP), p. 17
30. Hughes, D., et al. 1998, *Nature*, 398, 241
31. Kenefick, J. D., Djorgovski, S. G., & de Carvalho, R. R. 1995, *AJ*, 110, 2553
32. Lagache, G., et al. 1999, preprint (astro-ph/9901059)
33. Lanzetta, K. M., Wolfe, A. M., & Turnshek, D. A. 1995, *ApJ*, 440, 435
34. Leitherer, C., et al. 1995, *ApJ*, 454, L19
35. Lilly, S. J., et al. 1996, *ApJ*, 460, L1
36. Lilly, S. J., et al. 1998, astro-ph/9807261
37. Madau, P., Ghisellini, G., & Fabian, A. C. 1994, *MNRAS*, 270, L17
38. Madau, P., et al. 1996, *MNRAS*, 283, 1388
39. Madau, P., Haardt, F., & Rees, M. J. 1998, *ApJ*, in press
40. Madau, P., Meiksin, A., & Rees, M. J. 1997, *ApJ*, 475, 429
41. Madau, P., Pozzetti, L., & Dickinson, M. E. 1998, *ApJ*, 498, 106
42. Magorrian, G., et al. 1998, *AJ*, 115, 2285
43. Meurer, G. R., et al. 1997, *AJ*, 114, 54
44. Miralda-Escudé, J., & Rees, M. J. 1998, *ApJ*, 497, 21
45. Osmer, P. S. 1982, *ApJ*, 253, 280
46. Ostriker, J. P., & Gnedin, N. Y. 1996, *ApJ*, 472, L63
47. Pascarelle, S. M., Lanzetta, K. M., & Fernandez-Soto, A. 1998, *ApJ*, 508, L1
48. Pettini, M., et al. 1998, *ApJ*, 508, 539
49. Pozzetti, L., et al. 1998, *MNRAS*, 298, 1133
50. Rowan-Robinson, M., et al. 1997, *MNRAS*, 289, 490
51. Sawicki, M., & Yee, H. K. C. 1998, *AJ*, 115, 1329
52. Schmidt, M., Schneider, D. P., & Gunn, J. E. 1995, *AJ*, 110, 68
53. Schneider, D. P., Schmidt, M., & Gunn, J. E. 1991, *AJ*, 101, 2004
54. Shaver, P. A., et al. 1996, *Nature*, 384, 439
55. Songaila, A. 1997, *ApJ*, 490, L1
56. Steidel, C. C., et al. 1996, *ApJ*, 462, L17
57. Steidel, C. C., et al. 1998, *ApJ*, 492, 428
58. Steidel, C. C., et al. 1998, *ApJ*, submitted (astro-ph/9811399)
59. Tresse, L., & Maddox, S. J. 1998, *ApJ*, 495, 691
60. Treyer, M. A., et al. 1998, *MNRAS*, 300, 303
61. Warren, S. J., Hewett, P. C., & Osmer, P. S. 1994, *ApJ*, 421, 412
62. Williams, R. E., et al. 1996, *AJ*, 112, 1335
63. Soltan, A. 1982, *MNRAS*, 200, 115